IN SITU WAFER-LEVEL POLARIZATION OF ELECTRET FILMS IN MEMS ACOUSTIC SENSOR ARRAYS

M. Kranz[1], M.G. Allen[2], and T. Hudson[3]
[1]Stanley Associates, Huntsville, AL, USA
[2]Georgia Institute of Technology, Atlanta, GA, USA
[3]U.S. Army AMRDEC, Huntsville, AL, USA

ABSTRACT

MEMS-based electret transduction has been reported for both acoustic sensors and energy harvesters. Common techniques employed in MEMS electret formation include corona discharge [1] and backlighted thyratron [2]. This paper reports a method for post-release *in situ* polarization of electret films within a MEMS device. The method utilizes microplasma discharges with self-aligned charging grids integrated within the device to charge fluoropolymer films in a fashion similar to the corona discharge technique. This *in situ* approach enables the integration of uncharged electret films into MEMS and subsequent post-fabrication charging, simultaneously enabling the formation of buried or encapsulated electrets as well as eliminating the need to restrict fabrication processes that might otherwise discharge pre-charged electret materials. The method is applied to a single-chip array of acoustic sensors designed to capture and analyze waveforms from impacts.

KEYWORDS

Microplasma, Microcorona, Electret, Ultrasonic

INTRODUCTION

Electret Applications in MEMS

An electret is a material with a quasi-permanent electrostatic polarization. Electrets can be fabricated from multiple materials, with polymers being commonly employed. Polymer electret films can be used directly as a sensor [3, 4], or indirectly as a voltage bias [5, 6].

When used directly as a sensor element, changes to film geometry alter its electrostatic configuration. These changes can be amplified in applications such as strain sensing. Although employed in a fashion similar to piezoelectric materials such as PZT, BaTiO3, and LiNbO3, polymer electrets offer advantages including MEMS-friendly process flows and options for conformal and transparent coating.

In addition, the large remnant voltage seen across its surface allows electret application as a permanent voltage bias. This approach is used in electret microphones and energy harvesters, wherein the electret biases a movable structure. Acoustic waves or vibrations displace the structure with respect to the film, leading to current flow in an external circuit.

Electret Integration Challenges

In these applications, the use of electret films leads to challenges in overall device fabrication. In particular, the surface of the polymer must be exposed to the charging apparatus during the polarization process, thereby requiring the absence of fabricated structures above the film. Furthermore, once charged, significant discharge can occur if exposed to temperatures near the glass transition of the polymer, thereby limiting subsequent device fabrication to low-temperature processes.

As a result, most devices that employ active electret films are fabricated in two parts, one being a sensor component, and the other being a separate electret component. The electret can then be charged independently of the sensor fabrication. After completing fabrication of the two parts, they are assembled using a low-temperature process. However, it is often desirable to fabricate the entire device on one wafer, and perform electret formation after wafer completion. *In situ* charging approaches can fulfill this goal.

ELECTRET INTEGRATION APPROACH

Figure 1 shows electret charging based on the corona discharge apparatus. A needle with a 2 mm diameter tip is suspended 10 mm above the specimen. High voltage placed on the tip leads to ionization of the air near the tip. Charged species accelerate through a biased control grid towards the specimen, where they transfer charge to the surface. The large bulk resistivity of the polymer surface allows the charge to remain for long periods of time.

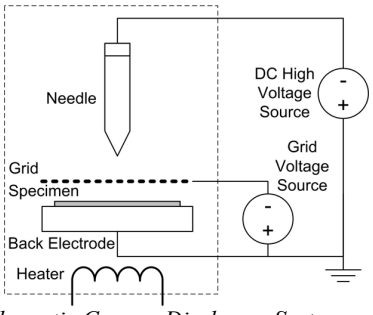

Figure 1: Schematic Corona Discharge System

Microcorona discharges have been previously achieved in microfabricated structures [7, 8, 9]. We demonstrate the use of this phenomenon for *in situ* charging of electrets and electret arrays. The *in situ* approach described here miniaturizes the traditional corona discharge apparatus, and embeds it within the sensor device itself. Figure 2 shows a cross-section of an *in situ* charging grid comprising multiple micro corona electrodes. These electrodes are conceptually similar to the corona wires in copy machines and laser printers.

They are suspended above the electret film using posts fabricated from the film itself. When energized, dielectric breakdown of the air in the gap leads to plasma discharges resulting in charge transfer to the electret film. This charging grid can be fabricated within the MEMS structure itself and electret polarization can occur after complete device fabrication and release.

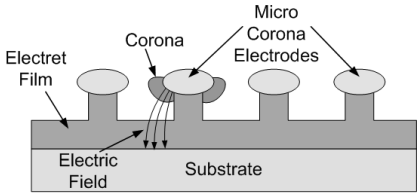

Figure 2: Miniature MicroCorona Sources

SENSOR CONCEPT

Figure 3 shows the sensor under consideration, consisting of a simple metal bridge suspended above a charging grid and polymer film. Once polarized, the electret film creates a voltage bias that capacitively couples with the suspended metal bridge. As the bridge experiences motion, a displacement current is generated in an external circuit. Figure 4 shows the layout of a full sensor chip consisting of multiple metal bridges, with lengths varying from 800µm to 2mm, suspended over an array of interconnected charging grids.

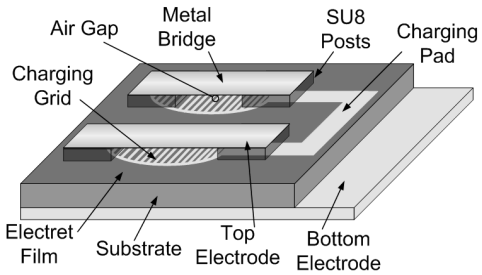

Figure 3: In situ *Polarized Electret-Biased MEMS Sensor*

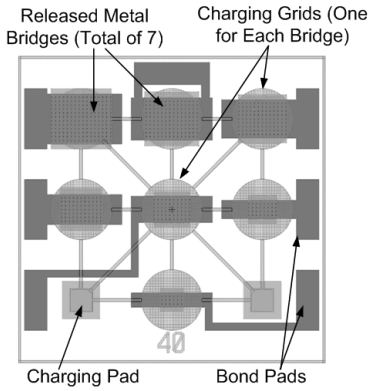

Figure 4: Layout of Entire Sensor Array

CYTOP [10], a thermoplastic fluoropolymer encapsulant for electronics, is used as the polymer electret because it can be spin-cast, has a high resistivity, and is easily etched in oxygen plasma. The grid structure is critical to the *in-situ* charging method. It consists of multiple thin-film metal edges suspended a short distance above the polymer film. When energized by a high voltage, the sharp metal edges lead to high dielectric fields that ionize the air in the gap and force electric charge onto the polymer surface. In this work, the grid consisted of an array of narrow lines, approximately 5µm wide, and separated by an approximately 40µm gap. The metal lines are suspended approximately 2µm above the polymer film through the simple fabrication process shown in Figure 5. The metal is first deposited directly on the polymer, patterned, and then "suspended" by isotropically etching the polymer out from underneath it.

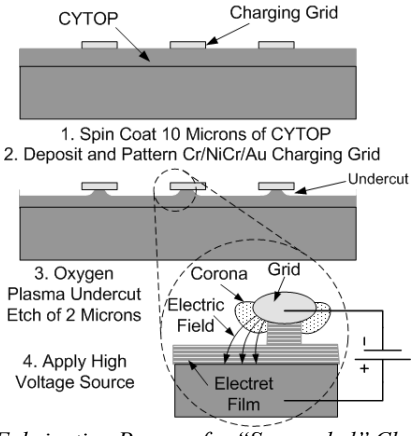

Figure 5: Fabrication Process for "Suspended" Charging Grid above Polymer Surface

After fabrication of the charging grid, additional microfabrication steps, as shown in Figure 6, are performed to build the acoustic sensor array [11]. SU8 is first spin-coated over the charging grids and a pattern of posts is exposed. The SU8 is not immediately developed, but instead undergoes a 12 hour post-exposure bake. After the bake, the wafer is coated with Cr using a low-power e-beam evaporator. The low-power deposition minimizes SU8 crosslinking during the deposition. Following Cr deposition, a layer of gold is deposited. A photoresist plating mold is then spin-coated and patterned, followed nickel electroplating. Finally, the photoresist mold and the undeveloped SU8 are removed using a series of acetone and developer baths, yielding a fully released structure. An SEM image of a final sensor device with a charging grid is shown in Figure 7.

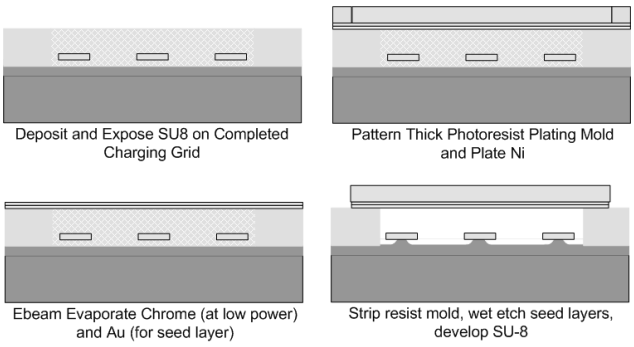

Figure 6: Sensor Fabrication Process

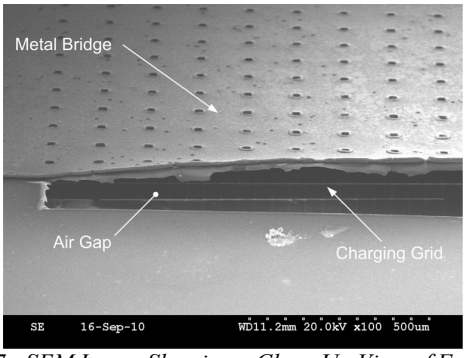

Figure 7: SEM Image Showing a Close-Up View of Fabricated Charging Grid

IN SITU CHARGING

After the MEMS structure is released, the electret formation process is performed by energizing the grid to a high negative voltage. When a suitable potential is achieved across the air gap between the grid and the polymer film surface, a microcorona discharge occurs. Ions travel to the polymer surface where they transfer their charge. The charge builds up until sufficient potential is achieved such that the microcorona no longer exists. Figure 8 shows the current through the grid structure during the charging cycle. The first peak represents charge being placed on the grid to raise its potential. The second peak represents the increase in current due to the onset of the microplasma discharge. Actual charged sites achieved an electrostatic voltage of approximately -200V after the first charging cycle when the grid was energized to -800V.

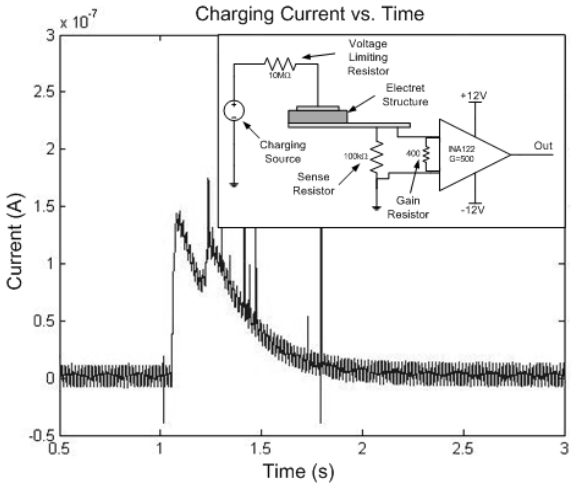

Figure 8: Measurement Circuit and Measured Current through the Structure during the First Charging Cycle

Figure 9 shows an optical image of the discharge event. The image on the left shows the charging grid as seen under normal lighting. The image on the right is of the same charging grid, but under no light conditions and captured during a portion of the discharge event. The intensity of the discharge is nonuniform across the charging grid and also time varying. This is due to nonuniformity of the metal edge sharpness, the orientation of the edge with respect to the polymer surface, and the actual gap between the edge and the polymer surface.

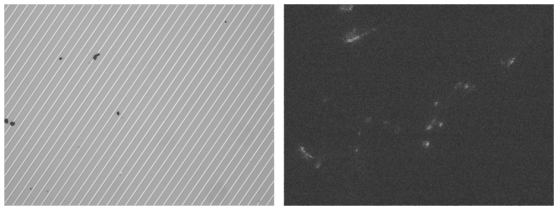

Figure 9: Optical Microscope Image of Discharge Process Showing Nonuniform Discharge Intensity

A field-nulling vibrating reed electrometer was used after polarization to measure the remnant voltage of each charging site. Figure 10 shows the achieved remnant voltage, after the application of -800V to the charging grid, plotted against the line spacing of the grid. Large line spacings resulted in higher remnant voltages as seen by the electrostatic voltmeter. This is due to the masking of the charge by the area of the metal conductors. The highest measured voltage results from the highest density of metal edges with the smallest total grid surface area.

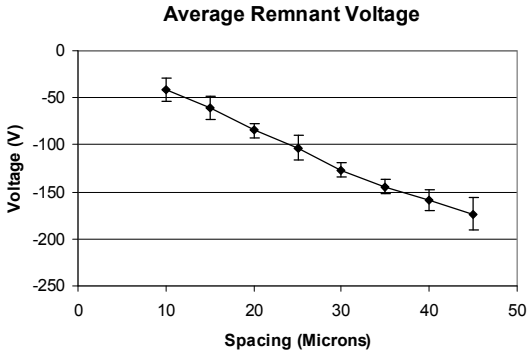

Figure 10: Average Remnant Voltage seen on Charged Sites of Varying Metal Spacing

Figure 11 shows the range of remnant voltages measured after polarizing multiple charging sites simultaneously on a single die. Each individual charging site is connected to the other charging sites and a contact pad. Upon application of the -800V charging potential, all sites are charged simultaneously.

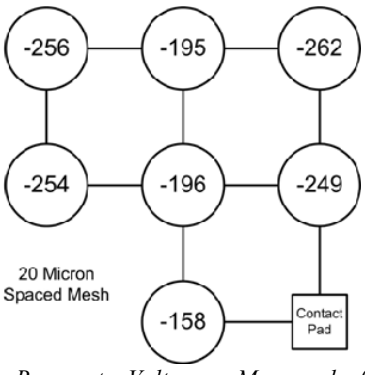

Figure 11: Remnant Voltages Measured for Multiple Simultaneous Charging Sites

SENSOR CHARACTERIZATION

A metal bridge transducer is suspended above each charging site; with each individual transducer in the array designed to exhibit a different natural frequency. This array was designed to perform spectral decomposition of an incident acoustic wave, with the natural frequencies spanning the range from 10kHz to 100kHz. When an impact or vibration is experienced, the output of the array represents a measurement of the spectrum of that input source. Figure 12 shows the sensor array attached to a hemispherical Alumina structure and impacted by a projectile. Four projectiles with identical geometries, but different materials, were dropped on to the hemisphere from a constant height. The materials used in the test were selected to provide a range of acoustic impedances, and included Teflon, acrylic, stainless steel, and silicon nitride.

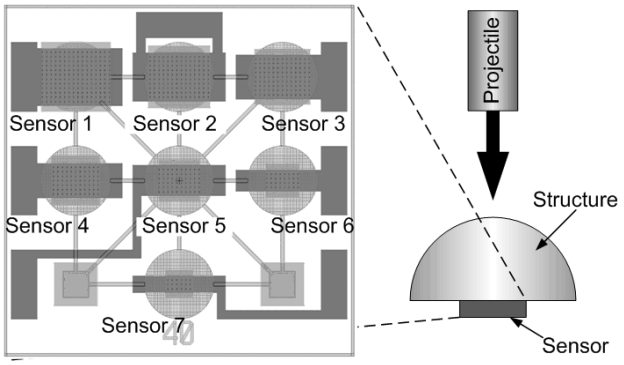

Figure 12: Sensor Array and Impact Test Setup

Figure 13 shows maximum peak voltage for each sensor from impacts between cylindrical projectiles of different materials and a ceramic hemi-sphere on which the sensor array is mounted. Each material presents a unique signature across the frequency spectrum. This sensor array demonstrates that *in situ* electret formation occurred within the structures, and that multiple sites could be charged with the application of voltage to a single contact pad, allowing the approach to be scaled to a full wafer implementation.

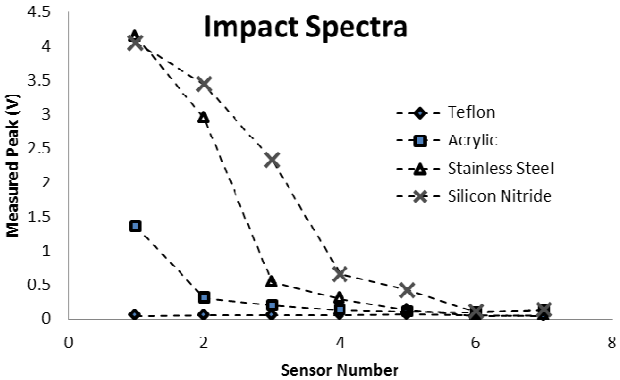

Figure 13: Output Spectra for Impacts with Different Materials

CONCLUSIONS

In situ charging of electret areas within a MEMS device is possible using microplasma discharges from a grid of thin film metal edges. The process can be performed after entire MEMS structure fabrication and release, thereby mitigating high-temperature process issues that electret films often experience. The process can also be scaled to the wafer-level.

REFERENCES

[1] Y. Arakawa, Y. Suzuki, and N. Kasagi, "Micro Seismic Power Generator Using Electret Power Film," *Power MEMS 2004*, Nov. 28, Kyoto, Japan.

[2] T. Y. Hsu, W. Hsieh, and Y. C. Tai, "A Thin-Film Teflon Electret Technology for Microphone Applications," *Tech. Dig. Solid-State Sensors and Actuators Workshop*, 1996.

[3] M. Goel, "Electret sensors, filters and MEMS devices: New challenges in materials research," Current Science, Vol. 85, No. 4, 25 August 2003.

[4] T.-H. Hsu, C.-N. Yeh, and Y.-C. Su, "Piezoelectric PDMS Electrets for MEMS Transducers," *IEEE MEMS 2010*, Hong Kong, January 25-28, 2010.

[5] T. Sterken, K. Baert, R. Puers, S. Borghs, "Power extraction from ambient vibration," *Proceedings of the Workshop on Semiconductor Sensors*, November 29, 2002, Veldhoven, the Netherlands, p. 680-683.

[6] E. Halvorsen, E. R. Westby, S. Husa, A. Vogl, N.P. Østbø, V. Leonov, T. Sterken and T. Kvisterøy, "An Electrostatic Energy Harvester with Electret Bias", *Transducers 2009*, Denver, CO, June 21-25, 2009.

[7] S. Lee, D. Kim, M. D. Bryant, F. Ling, "A Micro Corona Motor," Sensors and Actuators A, 118, 2005, pp. 226-232.

[8] C. G. Wilson and Y. B. Gianchandani, "Silicon Micromachining Using *In Situ* DC Microplasmas," Journal of Microelectromechanical Systems, Vol. 10, No. 1, March 2001.

[9] M. Honzumi, A. Ueno, K. Hagiwara, Y. Suzuki, "Soft-X-Ray-Charged Vertical Electrets and Its Application to Electrostatic Transducers," *23rd IEEE International Conference on MEMS (MEMS 2010)*, Hong Kong, January 2010.

[10] Y. Sakane, Y. Suzuki and N. Kasagi, "The development of a high-performance perfluorinated polymer electret and its application to micro power generation," Journal of Micromechanics and Microengineering, 18 (2008) 104011 (6pp) 29 September 2008

[11] C. Chung and M. Allen, "Uncrosslinked SU-8 as a sacrificial material," Journal of Micromechanics Microengineering, v.15, no.1, pp. N1-N5.

CONTACT

* M. Kranz, Stanley Associates, 7067 Old Madison Pike, Suite 100, Huntsville, AL, USA, 35806, Tel: +1-256-922-2378; Fax: +1-256-534-6473; E-mail: Michael.Kranz@stanleyassociates.com